lubricants

MDPI

Review

The Role of Solid Lubricants for Brake Friction Materials

Werner Österle [1,*] and Andrey I. Dmitriev [2,3]

1 BAM Federal Institute for Materials Research and Testing, 12200 Berlin, Germany
2 ISPMS Institute of Strength Physics and Materials Science, 634021 Tomsk, Russia; dmitr@ispms.ru
3 Department of Metal Physics, Tomsk State University, 634050 Tomsk, Russia
* Correspondence: Werner.oesterle@bam.de; Tel./Fax: +49-30-8104-1511

Academic Editor: Thomas W. Scharf
Received: 11 December 2015; Accepted: 19 February 2016; Published: 29 February 2016

Abstract: This review article comprises of three parts. Firstly, reports of brake manufacturers on the beneficial impact of solid lubricants for pad formulations are surveyed. Secondly, since tribofilms were identified to play a crucial role in friction stabilization and wear reduction, the knowledge about tribofilm structures formed during automotive braking was reviewed comprehensively. Finally, a model for simulating the sliding behavior of tribofilms is suggested and a review on modelling efforts with different model structures related to real tribofilms will be presented. Although the variety of friction composites involved in commercial brake systems is very broad, striking similarities were observed in respect to tribofilm nanostructures. Thus, a generalization of the tribofilm nanostructure is suggested and prerequisites for smooth sliding performance and minimal wear rates have been identified. A minimum of 13 vol % of soft inclusions embedded in an iron oxide based tribofilm is crucial for obtaining the desired properties. As long as the solid lubricants or their reaction products are softer than magnetite, the main constituent of the tribofilm, the model predicts smooth sliding and minimum wear.

Keywords: solid lubricant; friction; automotive braking; tribofilm; third body; sliding simulation; MCA modelling

1. Introduction

Solid lubricant nanoparticles like graphite, MoS_2 or WS_2 are frequently used as oil additives. Their beneficial role for friction and wear reduction under mixed lubrication regimes has been elucidated in several review articles recently [1–3]. Since the particles from which tribofilms form are so small, the film thickness usually amounts to less than 100 nm. Whereas under mixed lubrication conditions using additive-free engine oil the coefficient of friction (COF) of steel-on-steel contacts approaches 0.15, it drops well below 0.05 under hydrodynamic lubrication conditions [4]. The objective of using oil additives is to keep the ultra-low COF even under mixed lubrication conditions when asperities of the counter-bodies come into direct contact with each other [2]. This usually is achieved by crystallographically aligned solid lubricant films of either graphite [5–7] or MoS_2 and WS_2 [8–12], or by amorphous films which can flow in a fluid-like manner [13,14].

Whereas the mechanisms of superlubricity caused by solid lubricant films are fairly well understood nowadays, the role of solid lubricants as friction stabilizers in typical dry friction applications like brakes and clutches is not so clear. Doubtlessly, the formation of solid lubricant films would reduce friction to an extent which cannot be accepted during braking. Therefore, other mechanisms must be responsible for the desired effect of friction force stabilization at a medium COF-level in the range 0.3–0.5. For decades, the challenge was to develop brake friction materials

which, if rubbed against a cast iron rotor, provide smooth sliding and a stable COF within a wide range of stressing and environmental conditions. Therefore, it seems reasonable to start with a review on progress made with the addition of solid lubricants to brake pad formulations. A further literature review demonstrates how Godet's third body approach [15] is related to mechanisms occurring at the interface between the brake pad and disc. This section is dedicated to the characterization of tribofilms formed during automotive braking. Finally, modeling approaches enabling visualization of sliding mechanisms at the pad–disc interface, and providing an estimate of corresponding COF-evolution are reviewed.

2. Impact of Solid Lubricant Additions to Brake Pad Formulations

2.1. Why Do We Need Solid Lubricants for Brake Applications?

According to a report prepared by P. Blau for the U.S. Department of Energy, the first resin-bonded friction composites were developed already around 1950 [16]. From the beginning, brake pad materials were multiple composites and the number of ingredients increased continuously with the years. Complex materials are needed because of the multiple functionalities which have to be met. Constant friction within a wide range of stressing and environmental conditions is not the only criterion. Furthermore, the customer expects smooth pedal feel and noiseless braking operation. Especially the latter comfort requirements are a great challenge for brake and car manufacturers. The function of solid lubricant additions is to initiate smooth sliding conditions without impairing the frictional performance too much. Naturally, formulations become more and more complicated during an optimization procedure. This makes it almost impossible to assess the impact of one specific constituent on brake performance properties unless all stages of material development are known. Therefore, it makes sense to start the review while focusing on the literature describing systematic studies on more or less simple model materials, and then check whether the observed principles can be applied to more complex composites as well.

2.2. Addition of Graphite

Graphite is the most widely used solid lubricant for all kinds of applications including friction composites. Furthermore, it is present in almost every disc brake system in the form of graphite flakes as constituent of the cast iron rotor. As mentioned by Blau [16], its impact on tribological properties can be manifold, depending on structure variants, contaminants and environmental conditions. Pure graphite-like friction materials are applied as so-called C/C-brakes for aircraft braking. Since they always operate at elevated temperature, the problem of low friction at ambient conditions, especially under high humidity, can be neglected. Goudier *et al.* observed a low to high friction and wear transition at 300 °C which could be attributed to the onset of oxidation [17]. Kasem *et al.* observed a similar transition already in the temperature range 130–180 °C [18]. The same effect may also explain the results of Stadler *et al.* who reported on an increase of the COF and wear volume with increasing graphite content in the high temperature range, and an undesired low COF at ambient temperature in a metal matrix composite (MMC) pad rubbing against a C/C-SiC ceramic brake disc [19]. Cho *et al.* performed thermogravimetric analysis of graphite showing signs of oxidation not until 700 °C [20]. These authors also pointed out that flash temperatures at tribological contacts usually are much higher than average surface temperatures measured near the disc surface. Thus, tribooxidation of the graphite could have occurred readily under the applied conditions of testing. Nevertheless, in contrast to metal sulfide additions which will be discussed later, a positive effect of graphite towards friction stabilization at elevated temperatures was not proved in this case. This may be due to the fact that a graphite-free reference material was missing, or, that the composition of the friction material was already too complex. The same holds for a recent study by Ram Prabhu, who also could not elaborate a clear effect of graphite addition to a MMC friction material in contrast to MoS_2 addition [21]. There are some other studies on copper-based MMCs which show clear effects of graphite additions on triboligical

properties [22,23]. The observed effect was a decrease of COF and wear with increasing graphite content. An interesting finding was that a major amount of the wear debris consisted of iron oxides [22]. A systematic investigation considering well-defined powder mixtures of copper and graphite showed a transition from a high to a low friction regime with increasing graphite concentration [23]. At 10% graphite, which is a common number of brake friction materials, the system was in the high friction regime corresponding to a COF of 0.5. However, even for pure graphite powder, the COF was still near to 0.3 which is much higher than the one observed for the C/C couple at ambient temperature (0.15) [17,18]. Although not designed for brake application, it is interesting to look at the results obtained with epoxy coatings filled with graphite and MoS_2 particles [24,25]. While rubbed against steel discs, the pure epoxy provided a COF of 0.5 and 0.55, according to [24] and [25], respectively. Epoxy filled with at least 10 wt % graphite provided a COF of 0.35 which remained constant with increasing graphite content [25] or decreased slightly to 0.25 [24]. If we assume that the graphite particles are released from the film during the tribological test, forming a graphite particle layer at the interface, the COF should be lower. An explanation for the observed higher COF is that the released graphite particles mix with iron oxide particles formed by tribooxidation of the steel disc. The sliding behavior of iron oxide mixed with different concentrations of graphite was studied comprehensively by modelling, as described in Section 4.

2.3. Metal Sulfide Based Solid Lubricants

A number of metal sulfides are frequently applied in brake pad formulations, although rarely as single additives. The functionality of these constituents is to provide friction stability and to reduce wear at elevated temperatures. It was assumed that chemical reactions occurring at these elevated temperatures are responsible for the beneficial effects, and therefore Melcher and Faullant studied the thermo-physical properties of a comprehensive number of candidate materials and their oxides [26]. Some of their findings are the following: Classical solid lubricants with a layer structure are besides graphite and hexagonal BN: SnS_2, WS_2, TiS_2 and MoS_2. Other soft sulfides with Mohs hardness 2 or less but without layer structure are: Sb_2S_3, SnS, Bi_2S_3 and CuS. Some of the latter are also frequently used as friction modifiers indicating that a layer structure is not a necessary prerequisite for obtaining the desired brake performance properties. According to Melcher and Faullant [26], such desired properties may be linked to phase transitions and/or chemical reactions and the properties of reaction products. The authors described some scenarios that could happen with the different additives during braking, but their experimental studies were not adequate for providing proof for their assumptions. Nevertheless, they compared a large number of different solid lubricant additions (6 wt % each) with a so-called base-formulation, and they could show impacts on wear and COF at 100 °C and 400 °C. Similar results were obtained by Hoyer *et al.* by adding 8 vol % of CuS_2, PbS or Sb_2S_3 to three different types of base compositions [27]. Matejka *et al.* observed a chemical reaction of Sb_2S_3 with iron [28] at 350 °C and correlated this with the observed decrease of the COF. According to these studies, each additive provided positive and negative effects. Therefore, a coherent conclusion is that single additives cannot fulfill all requirements, and that a combination of different ingredients is needed. Systematic approaches with different solid lubricant combinations were described by Jang and coworkers for graphite/Sb_2S_3 [29] and graphite/Sb_2S_3/MoS_2 [20,30]. There are some commercial products on the market promising smooth sliding without reducing the COF. One paper is pointing out that the perfect additive consists of graphite particles coated with molybdates, phosphates, sulfates or sulfides [31]. The authors claim having obtained achievements by using such additives in a brake pad formulation, but such results cannot be generalized without knowing the mechanisms behind the observed effects.

As already mentioned above, it is almost impossible to predict the impact of single ingredients on brake performance properties of commercial friction materials, which further differ enormously in their base compositions. Nevertheless, we can learn from the experiences made by friction material compounders. Some of the numerous observations made during material development

and dynamometer testing are compiled in Table 1. Only major components neglecting fillers are given in column 1. The term fade means decrease of COF at elevated temperatures. COF_1 indicates the COF-range obtained during moderate braking and COF_2 the friction behavior observed during typical fading cycles. If different material variants were considered within one study, the optimized composition in respect to overall brake performance was selected for displaying the COF data.

Table 1. Literature review on the impact of solid lubricant additions to commercial brake pad formulations.

Friction Material and Rotor Material If Other than Cast Iron	Tested Variable	Observations/Ref.	COF_1 COF_2
vol %: fibers 23, organics 23, sulfides 8	Metal content: 0%, 9%, 14%	Metal-free: highest wear; no systematic impact of sulfides, but Sb_2S_3 and PbS better than Cu_2S [27]	0.4 0.4
vol %: fibers 12, organics 33, solid lubs. 10–14, abrasives2–6	Sb_2S_3: 2–6 $ZrSiO_4$: 6–2	Formation of Sb_2O_3 stabilizes COF; $ZrSiO_4$ prevents fade [30]	0.3 0.4
Non-asbestos organic pads (no details on base composition)	13 different sulfide additions 6 wt % each	SnS/SnS_2 blend recommended as substitute for Sb_2S_3 [26]	0.4–0.5 0.35
vol %: fibers 22, organics 28, solid lubs. 13, abrasives 1.5/3	Graphite: 10/11 Sb_2S_3: 3/3.5 $ZrSiO_4$: 3/1.5	Optimum performance for combination of 11% graphite, 3.5% Sb_2S_3 and 1.5% $ZrSiO_4$ [32]	0.65 no data
wt %: no fibers but Cu particles 15–25, organics 25, graphite 5	Cu particle size	Anomalous COF: increasing with temperature [33]	0.2–0.3 0.4–0.5
vol %: fibers 13 (aramid + ceramic), resin 18, solid lubs. 10	Graphite/Sb_2S_3/MoS_2 different ratios	7 Graphite + 3 Sb_2S_3 best fade resistance and lowest wear [20]	0.45 0.5
vol %: fibers 17, organics 40, solid lubs. 18, abrasives 4	Graphite: 0–9 Sb_2S_3: 9–0	Both solid lubs. needed. Best performance: graphite 6, Sb_2S_3 3 [29]	0.35 0.42
vol %: fibers 21, resin 35, solid lubs. 0–25, abrasives 4	0%, 5%, 10%, 15%, 20%, 25% of either talcum, h-BN or petroleum coke	Best performance properties with 10 vol % h-BN [34]	0.45 0.45
P/M pad against C/C-SiC disc wt %: metal particles 84–100, graphite 0–15, abrasives 0–5	Metal 100 Metal 85/graphite 15 Metal 95/SiC5	Effect of graphite : increased COF (0.6) and wear [19]	0.4–0.5 0.3–0.6
P/M pad against steel disc wt %: metal particles (Cu) 90 Solid lubs. 10, abrasives 6 (SiC)	Graphite/h-BN ratio	With increasing graphite content COF/wear decreased. Graphite + h-BN stabilized COF [22]	0.4–0.5 no data
wt %: fibers 33, resin 10, graphite 10, abrasives?	Graphite particle size	COF decreased with increasing particle size [35]	0.45 no data
wt %: fibers 33, resin 10, graphite 10, abrasives not specified	Graphite particle size	Best performance for lowest particle size (21 µm) [36]	no data 0.3–0.4
vol %: fibers 6–11, organics 45, solid lubs. 10, coke 14–17 abrasives 2–5	Towards eco-friendly: Cu-free, Sb_2S_3-free, no ceramic whiskers	Combination of 14 coke, 10 graphite and 0.4 MoS_2 provided good brake performance [37]	0.4–0.5 0.3–0.4
vol %: fibers 50, organics 35, solid lubs. 4.8 (Sb_2S_3 only), abrasives 0/5.6	Al_2O_3 content: 0% and 5.6%	Overall higher COF with Al_2O_3. Unexpected fade ascribed to Sb instead of Sb_2O_3-formation [28]	0.3/0.5 0.2/0.4
P/M pad against cat iron disc vol %: metal particles 80 (Cu), solid lubs. 10, abrasives 10	Type of solid lub. either graphite, h-BN or MoS_2	Ranking for best brake performance: MoS_2 > graphite > h-BN [21]	0.2–0.3

Considering all observations together, the following general conclusions can be drawn. Solid lubricants are needed to provide a constant COF within a range of 0.3–0.5, irrespective of the applied load and sliding velocity at moderate and elevated temperatures. The concentration of solid lubricant additions must not exceed a certain limit of approximately 10 vol %, because otherwise the COF might drop below 0.3. Using only one type of a certain solid lubricant usually does not yield satisfactory results. Frequently, a combination of graphite and one of the soft metal sulfides is the

best choice. Since the sulfides usually are oxidized at elevated temperatures during fading cycles, the evolving oxides should have similar mechanical strength as the original ingredients. In fact, this prerequisite is only fulfilled strictly for Sb_2S_3 and PbS. Since both raw materials should be replaced in brake pad formulations because of health concerns [38], other soft metal sulfides have been tested comprehensively. Their oxides, like MoO_3, SnO, Bi_2O_3 and CuO, are harder than the corresponding sulfides, albeit still softer than the iron oxides [26]. The latter finding will be important for the discussion in Section 5. Although most brake pad manufacturers have reduced or eliminated Sb_2S_3 from their formulations, published reports on systematic studies with the other sulfides are still rare. As discussed during recent brake conferences [39–41], tin sulfides are currently regarded as the most promising candidates for antimony replacement in brake pad formulations. A recently published paper shows that good friction properties had been achieved with a solid lubricant blend consisting of tin sulfide, iron sulfide and potassium titanate [42]. Certainly, tin sulfide is not the only alternative to Sb_2S_3. Yun *et al.* prepared an eco-friendly brake friction material without copper, lead, tin, antimony trisulfide and whisker materials [37]. They used a small amount of MoS_2 in combination with graphite to reach this goal.

Most authors cited in Table 1 state that the formation of a stable tribofilm is responsible for achieving the desired brake performance properties. Exact knowledge about the structure and properties of such films seems to be the key for understanding the friction and wear behavior of the frictional brake system. Therefore, the state of the art of tribofilm characterization in conjunction with braking is reviewed in the next section.

3. Structure and Composition of Tribofilms Formed during Braking

Since almost 50 years, attempts were made to characterize and understand the material changes occurring at the interface between a rotating brake disc sliding against a fixed pad, the latter consisting of a friction composite. Whereas in at least 90% of considered studies the rotor material was the same, namely grey cast iron, the composition of the tested friction composites varied enormously. However, every commercial brake friction material has to fulfill similar requirements in terms of friction level, friction stability and wear with only slight differences in preferences according to the car manufacturers. This suggests that the composition and microstructure of wear products, which are partly released to the environment and partly forming tribofilms if compacted and bonded to the first body surfaces, should have similar microstructures which determine their friction and wear behavior while sliding against each other. Investigations performed by the authors during the last 15 years revealed a lot of details concerning tribofilm structures. In the following, the results are discussed in the context of a comprehensive, although certainly not complete, literature-review. The only restriction made during preparing the review was that the considered wear products were formed under real braking conditions leading to a COF level in the range of 0.3–0.5 (see also Table 1). The results of the review are compiled in Table 2. Naturally, the completeness of the derived information depends on the applied characterization methods. Therefore, usually only partial information was available within one study, which sometimes caused misinterpretation of the results by the authors. Therefore, whenever reasonable, an attempt was made to reinterpret the results in the light of the numerous new findings published in the meantime. The meanings of acronyms for the different methods are given in Table 3.

Table 2. Literature review on the characterization of tribofilms observed after brake dynamometer testing, and corresponding methods (chronological order).

Reference	Methods	Observations	Authors' Interpretation	Comments
[43] 1973	LM TEM	Much less coarse and fine asbestos fibers observed, as expected.	Most asbestos converted to olivine and stored at surface as tribofilm.	Olivine mixed with other wear products has formed a tribofilm.
[44] 1973	EA TGA PGC	Thermal degradation of phenolic resin during braking.	Formation of a residual polymer which is aromatic hydrocarbon in nature.	Formation of a soft solid state wear product which is mixed with other wear debris.
[45] 1978	SEM EDS XRD	Mix of debris from pad and rotor forming tribofilms. Reduction of Fe and graphite grain size (XRD). Enrichment of inorganic species near pad surface.	No oxide observed at low temperature attributed to continuous removal. Plastically deformed layer and transferfilm at disc surface identified.	Almost all interpretations consistent with most recent findings. Exception: no iron oxide observed at low temp. This may be due to very thin tribofilm.
[46] 1978	X-LM TGA XRD XFA	Changes of tribo-affected zone with increasing temperature: More inorganic, less asbestos, less polymer species.	Increasing wear with increasing temperature, complex material changes. Black tribofilm interpreted as carbonaceous material	Black tribofilm at elevated temperatures consists of magnetite mixed with carbonaceous material.
[47] 1980	LM SEM EDS MH	Wear particles consisting of iron and iron oxide. Cu transfer to disc.	Formation of metallic iron and copper was attributed to hydrogen evolution during resin degradation.	Observations confirmed by later studies. Role of hydrogen not confirmed.
[48] 1989	LM SEM PGC	Incompletely oxidized metal and graphites. 430 °C wear debris contained degraded resin.	Tribofilm continuously formed by compaction of wear debris, and sheared on both counterbodies.	This interpretation is up to date.
[49] 1994	XPS EDS	MoS_2 and Ba SO_4 not stable but transformed to MoO_3 and BaO, respectively.	Although, transferfilm chemistry depends on abrasive addition, little effect on friction and wear.	MoO_x confirmed [50] BaO not confirmed by additional studies.
[51] 1999	LM SEM EDS TEM-ER	Tribofilm from wear debris. 3rd body differs from original materials. Aramid-based tribofilm.	Good coverage of surface with tribofilm formed from wear debris provides wear protection.	The general conclusion is correct. The role of aramid for tribofilm formation not confirmed by further studies.
[27] 1999	SEM EDS AES	Occasional transfer of pad material to disc. FeO and C at the surface (AES).	No tribofilm formed at low temperature, only at high temperature (SEM/EDS).	Thin tribofilms not detected by SEM/EDS. FeO not confirmed. State of the art: Fe_3O_4.

Table 2. *Cont.*

Reference	Methods	Observations	Authors' Interpretation	Comments
[52] 2000	SEM OP IIT	Primary and secondary contact plateaus. Ultra fine-grained top layer. High hardness of this layer.	Wear particle flow between protruding plateaus. Compaction and tribo-sintering of particles. FeO and/or Fe_3O_4 (EDS). No signs of C in tribofilm.	State of the art description of the contact situation on the µm-scale Misinterpretation of nanoscale features (appl. methods not appropriate).
[53] 2000	PSF ELPI EAA PIXE	Significant fraction of airborne wear particles has diameters <100 nm. Fe was major element of sampled particles.	"Fiber emissions are not a concern", because of decomposition. Hydrocarbons may be ejected at higher temperatures.	Since O was not measured by PIXE, Fe_3O_4 nanoparticles are not only the major species of tribofilms, but also of airborne dust.
[54] 2001	LM at glass disc	Particle flow visualized.	*In-situ* observation of secondary contact creation.	Previous hypotheses confirmed
[55] 2001	SEM EDS X-TEM SAED XPS	Major species of tribofilm: Nano-barite mixed with other pad constituents (alloyed barite).	Hard ingredients like quartz served as primary plateaus. Barite-based 3rd body material forms secondary plateaus.	The unconventional pad material contained 48% barite. Barite-based tribofilm is not typical for commercial pad materials.
[55] 2002	LM GA-XRD X-SEM TEM-ER EDS	Heterogeneous tribofilm containing fragments of all pad constituents and reaction products in a matrix of Fe- and Cu-oxides. TEM revealed crystalline carbonaceous film (<10 nm thick).	Tribolayer consisting of fragments of pad ingredients in Fe/Cu-oxide matrix covered with carbonaceous tribofilm.	Fe-oxide based tribolayers confirmed by many other studies. Cu-oxide rarely observed, but rather metallic copper particles. Nanocrystalline carbonaceous film not confirmed. Could have been confused with nc magnetite-based film.
[56] 2002	TEM	Particles scratched from pad surface after braking tests. Nanocrystalline iron oxide (Fe_2O_3) identified.	Tribooxidation of disc and steel fibers and transformation of asbestos to olivine has occurred during braking.	Fe_2O_3 was not confirmed as major phase during subsequent studies, but rather Fe_3O_4.
[57] 2004	SEM EDS TGA	Wear particles of real brake sampled on filter show all pad constituents as well as Fe or Fe-oxide.	Wear product coinsists of fragmented constituents (pad), Fe-oxide from disc and degraded resin.	SEM/EDS revealed the coarse fraction of the wear debris and Fe-containing agglomerates of the fine fraction.
[58] 2004	DLS SEM EDS	Bimodal size distribution (nano/micro) of wear particles deposited near the friction couple. Nano fraction: high concentration of Fe, O, C.	Sub-micron particles: wear product of disc. Micron-sized particles: wear product of pads.	Agglomerates of fully processed third body consist mainly of iron oxide. Micron-sized particles represent early stages of pad wear.

Table 2. *Cont.*

Reference	Methods	Observations	Authors' Interpretation	Comments
[59] 2004	LM SEM/EDS FIB/SIM X-SEM X-TEM	Areas covered by nc-tribofilm on pad revealed in bright contrast in SIM. Tribofilm and wear particles mainly consist of iron oxides; Cu-oxides rarely observed; Cu and Zn-transfer to disc.	Tribooxidation of metallic constituents provides the major part of wear debris and tribofilm. More Cu- and less Fe-oxide at pad surface; the other way round for disc. Zn provides film adhesion.	Fe-oxides confirmed. Role of Cu-oxides not clear. Role of Zn transfer not confirmed, most likely over-estimated.
[60] 2004	LSM SIM	Contact areas identified by SIM are smooth areas, but not clearly identified as protruding plateaus.	Not only the protruding plateaus, but also deeper areas may have been contacting areas.	This interpretation did not consider flow of 3rd body particles and the possibility of particle trapping in troughs.
[61] 2005	X-SEM ERM	Transfer layers in a thickness range 10–50 μm were obtained by drag tests at elevated temperatures.	Solid lubricants exert great impact on transfer layer thickness. No effect on COF but smoother sliding.	The formation of such thick transfer layers is rarely observed in practice.
[62] 2006	SEM EDS XFA	Examples of binding solid lubricants to meso-scale pad constituents observed for commercial pad materials.	Distribution and retention of solid lubricants at the pad surface is an important issue.	Ingredients must be available everywhere at the rubbing interfaces for being incorporated into the 3rd body.
[63] 2006	FIB/TEM GDOS RS	Fe_3O_4-based tribofilm also contains amorphous and graphite-like C (RS). Ca-, S- and Cu-transfer to disc (GDOS).	Tribooxidation of Fe- constituents and mixing with graphite and other solid lubricants occurs on the nanometer scale.	Ca-enrichment at the disc surface not reported by other studies, except one [34].
[64] 2007	TGA MS SEM	Oxidation of resin into volatile species at 300–600 °C. Mechanical activation lowers temperature range.	Good friction performance even at high temperatures attributed to 3rd body layers formed during degradation of resin.	Obviously, secondary plateaus were retained at elevated temperatures (SEM).
[34] 2007	SEM EDS	EDS-maps suggest more material transfer from pad to disc for formulations with addition of sol. lubs.	The observed material transfer stabilized the COF and led to reduced wear.	Obviously an unconventional $CaCO_3$-based film has formed, because of high $CaCO_3$-content of the pad.
[65] 2007	FIB/SIM TEM/EDS	Plastically deformed layer below tribofilm at disc surface. Nc Fe_3O_4-based tribofilm mixed with small amount of pad constituents.	Mixing of Fe_3O_4 with soft nanoparticles from pad ingredients is a prerequisite for obtaining smooth sliding conditions.	This finding defined the basic structure for modelling the sliding behaviour of tribofilms, as discussed in Chapter 3.

Table 2. *Cont.*

Reference	Methods	Observations	Authors' Interpretation	Comments
[66] 2008	X-LM X-SEM GA-XRD	Zone of severe plastic deformation. Discontinuous tribofilm 3rd body mainly Fe-oxide Transfer of reaction products to disc surface.	Since nanocrystalline wear particles were observed, their potential risks have to be considered in the future.	Identification of reaction products at disc surface by GA-XRD not confirmed by further studies.
[67] 2009	LM X-SEM EDS FIB EF-TEM	Cross-section with pad still pressed against disc showed continuous 3rd body layer. Nasnoscale elemental mapping revealed C and Cu nanoparticles and submicron-sized Al_2O_3.	More 3rd body present at the interface while the pad is still pressed against the disc than usually observed during post mortem studies.	Complicated 3rd body structure with different submicron- or even micron-sized particles (depending on the thickness of the tribofilm) embedded in multi-phase nc-matrix.
[68] 2009	SMPS TEM EF-TEM HR-TEM	Nanoparticle emissions correlated with fading cycles. Nanostructure of collected dust particles.	Most pad constituents and Fe_3O_4 observed in a single nanoparticle of approximately 300 nm diameter.	Final state of 3rd body formation leads to mixing of wear products on the nanometer scale
[69] 2009	SEM	Cavities formed around steel fibers which then were filled with wear debris under dry conditions and with water under wet conditions.	COF-increase with pressure attributed to increase of real contact area. COF-decrease under wet conditions attributed to wear debris removal and mixed lubrication.	The study shows that mechanisms taking place at the meso- and micro-scale have to be kept in mind.
[70] 2010	PSS MöS TEM FTIR TGA	Submicron-sized wear particles detected. Fe^{2+}, Fe^{3+} and Fe^0 Core-shell Fe-Fe_3O_4-particles in matrix of amorphous carbon. Resin degradation observed. Resin degradation confirmed.	C-based ingredients (graphite, resin, coke . . .) all transformed to amorphous C, thus explaining the high fraction of amorphous carbon in the wear product.	The high amount of amorphous carbon in the wear product was not corroborated by other studies. Actually the investigated formulation contained much C. On the other hand, TEM always considers only very small volumes, and thus uncloses the danger of over-interpretation.
[37] 2010	SEM EDS	Different pad materials all covered with Fe-oxide based tribofilm.	Cu- and Sb-free pad forms similar tribofilm as conventional materials.	
[71] 2010	TEM/EDS EF-TEM HR-TEM	Nc- and multiphase-structure of Fe_3O_4-based tribofilm revealed.	Smooth sliding attributed to tribofilm structure, as shown by modelling.	Contrary to [70], it was observed that Fe_3O_4 is the matrix which contains C inclusions.
[72] 2010	EEPS CI EF-TEM STEM EDS	Airborne particles down to diameters of some few nanometers detected. Collected particles are agglomerates of nanoparticles of pad ingredients and Fe_3O_4.	Differences of pad formulations mirrored in differences of composition of nanoparticle-agglomerates.	Nanostructure and composition of airborne dust particles provide information of tribofilm structure.

Table 2. *Cont.*

Reference	Methods	Observations	Authors' Interpretation	Comments
[73] 2010	FIB TEM EF-TEM	Cu- and barite-nanoparticles (100 nm) embedded in Fe_3O_4-matrix.	Similar COF-stabilization effect of Cu-nanoparticles as graphite nanoparticles shown by modelling.	
[74] 2011	GA-XRD RS X-FIB EF-TEM HR-TEM	Fe_3O_4 on rubbed disc, disordered graphite, graphite lamella, exfoliated nano-graphite and graphite embedded in Fe_3O_4 observed.	Shear-induced crack at graphite-pearlite interface provides access of O thus enabling Fe_3O_4-formation, graphite nanosheet exfoliation and embedding.	This is only one mechanism of formation of graphite-like species.
[75] 2011	STEM/EDS HR-TEM X-TEM	Further example of Fe_3O_4-based tribofilm. Thick film consisting of 3 layers, formed during fading cycle.	Soft nanoinclusions in brittle Fe_3O_4 matrix provide smooth sliding.	
[28] 2011	SEM/EDS GA-XRD	Besides Fe_3O_4-based 3rd body, also Sb-sulfide and Sb-Fe particles were observed at pad surface.	The results suggest reduction of Sb_2S_3 to metallic Sb and alloying with Fe.	Unusual finding, not confirmed by other studies.
[76] 2012	EF-TEM HR-TEM	Extension of [73]. Cu, barite and zirconia nano-particles embedded in Fe_3O_4. Magnetite and graphite nanocrystals shown by lattice fringes.	Not only soft, but also hard nanoinclusions (ZrO_2) identified in a tribofilm formed by dynamometer testing.	
[77] 2013	SEM EDS	Transfer of barite, Cu and Zn from pad to disc.	The film consists of milled and compacted wear debris of the pad.	Most likely, the film consists mainly of Fe_3O_4; separation from strong Fe-peak of substrate not possible by SEM/EDS.
[78] 2014	FIB/SIM ATB-KT	Example of film built from powder particles. COF of Fe_3O_4 + 15% graphite: 0.25 and Fe_3O_4 + 15% graphite + 5% SiC: 0.35.	Artificial third bodies are useful for systematic studies on pad formulations and for verification of modelling results.	
[40] 2014	SEM/EDS FIB/X-SEM	Fe, C, O, S, Mg, Ba, Zn, Sn, Si, Al all observed at rubbed pad surface.	Reaction of metal powders with solid lubricants considered as beneficial.	Reaction products could not be identified unambiguously with the applied methods.
[42] 2015	SEM X-SEM EDS XRD	Fe-Zr mixed oxides in films and wear debris. XRD: mainly Fe_2O_3, also metallic copper.	Released and fragmented hard particles from pad mixed with Fe-oxide from disc. Cu needed for binding constituents of the tribofilm together.	In principle in accord with previous findings, but hematite instead of magnetite is unlikely, because of the black colour of brake dust.

Table 3. Definition of acronyms used for the characterization methods mentioned in Table 2

Acronym	Method
AES	Auger Electron Spectroscopy
ATB-KT	Artificial Third Body-Kato Test
CI	Cascade Impactor
COF	Coefficient of Friction
DLS	Dynamic Light Scattering
EA	Elemental Analysis
EAA	Electrical Aerosol Analyser
EDS	Energy Dispersive X-ray Spectroscopy
EEPS	Engine Exhaust Particle Sizer
EF-TEM	Energy-filtered TEM
ELPI	Electrical Low Pressure Impactor
ERM	Electrical Resistance Measurement
GDOES	Glow Discharge Optical Emission Spectroscopy
GA-XRD	Grazing Angle X-ray Diffraction
FIB	Focused Ion Beam
FTIR	Fourier Transform Infrared Spectroscopy
HR-TEM	High Resolution Transmission Electron Microscopy
IIT	Instrumented Indentation Testing (Nanoindentation)
LM	Light Microscopy
LSM	Laser Scanning Microscopy
MH	Micro Hardness
MS	Mass Spectroscopy
MöS	Mössbauer Spectroscopy
Nc	Nanocrystalline
OP	Optical Profilometry
PGC	Pyrolisis Gas Chromatography
PIXE	Proton Induced X-ray Emission
PSF	Particle Sampling on Filter
PSS	Particle Sampling by Sweeping the test chamber
RS	Raman Spectroscopy
SEM	Scanning Electron Microscopy
SIM	Scanning Ion Microscopy
SMPS	Scanning Mobility Particle Sizer
STEM	Scanning Transmission Electron Microscopy
TEM	Transmission Electron Microscopy
TEM-ER	Transmission Electron Microscopy of Extraction Replica
TGA	Thermogravimetric Analysis
XFA	X-ray Fluorescence Analysis
X-LM	Cross-sectional LM
X-SEM	Cross-sectional SEM
X-TEM	Cross-sectional TEM
XPS	X-ray Photoelectron Spectroscopy
XRD	X-ray Diffraction

At first, commonalities of the findings compiled in Table 2 are considered. Not a single case of a mono-phase solid lubricant film was observed. This clearly shows that the mechanism of friction stabilization at a medium COF-level is different compared to classical solid lubricant applications. In the latter case, the formation of a textured film providing easy shear planes leads to reduction of COF and wear. Furthermore, it was quite clear from the beginning that if films were observed at the surfaces of the first bodies, these were formed by compaction of wear products. Thus, it is quite clear that Godet's concept of a third body screening the surfaces of first bodies, pad and disc in our case, is valid [15]. Naturally, wear debris is formed by fragmentation and mixing of first body materials, and eventually by chemical reactions between different species and the atmosphere. Almost all studies provide evidence that such processes have occurred, although the degree of fragmentation and mixing can differ considerably from site to site on a rubbed surface. The findings also depend on

the applied characterization methods. Thus, LM and SEM will reveal fragments on the micrometer scale, while TEM is capable of revealing nanostructures but usually neglects or does not realize features on the micrometer scale. Since commercial brake pads generally consist of more than 10 ingredients, which furthermore differ in size, a large variety of different wear particles will be formed initially. The bigger particles cannot form stable films. Thus, they are either fragmented further or emitted to the environment. Under certain conditions several microns thick films were observed [61,75], although usually tribofilm thickness is in the sub-micron range. The latter films can only be formed from nanoparticles and, therefore, their structure can only be revealed by TEM-related methods. Nevertheless, SEM/EDS, XRD and some other bulk methods can provide information about third body composition and phase content provided that the third body material can be separated from its substrate. Considering these prerequisites, the majority of the studies of Table 2 led to the conclusion that the major phase of the third body, which finally is forming tribofilms, is iron oxide Fe_3O_4. Although Fe_2O_3 may sometimes form as well [42,56], there is strong evidence that Fe_3O_4 is the major phase for the following simple reason: If one touches a used brake pad or disc, the finger will turn black. Color is very sensitive to the type of oxide. Fe_3O_4 (magnetite) is black and Fe_2O_3 (hematite) is reddish or at least brown. Although, mostly only revealed by TEM-techniques, the nanocrystalline structure of the fully processed third body contains other species besides Fe_3O_4. Theoretically, all ingredients of the pad formulation or their chemical reaction products should be homogeneously mixed on the nanometer scale, provided the original ingredients are prone to nanostructure formation by mechanical processes like severe shear deformation or impact during particle collisions. The latter can be checked by ball milling experiments, as proved by several papers [70,79–81]. A special mechanism of nanostructure formation is tribooxidation of the cast iron disc providing the major constituent of the third body. Here, it is not only severe plastic deformation, but also the development of flash temperatures especially at the graphite lamellae which promote local magnetite formation and mixing with exfoliated graphite nanoflakes, as evidenced in [74]. Taking into account that other pad constituents may also provide nanoparticles which can be incorporated into the magnetite-graphite blend, the complicated EDS-spectra usually obtained from third bodies prepared for TEM-investigations can be explained. Whereas some ingredients, like magnetite and graphite are milled down to crystal sizes <10 nm, others, like copper or zirconia, are not fragmented further beyond approximately 100 nm [76]. The metal sulfides belong to the first category, because they never were observed as particles of the size class 100 nm within a fully processed third body. On the other hand, small but significant signals from Sb, Sn or other metal sulfides were frequently observed in EDS-spectra from third bodies indicating that species <10 nm containing such elements are present. This implies that the metal sulfides or their oxidation products are mixed with magnetite on the nanoscopic scale, similar to graphite.

Examples of the nanostructures described above can be viewed in previous articles [71–73,75,76]. A further not yet published example of a TEM study of a typical third body formed during braking with a commercial pad is shown in Figure 1. The nanocrystalline nature of this tribofilm is revealed by the TEM micrograph in Figure 1a. The film is embedded between an artificially applied platinum layer at the top and the plastically deformed cast iron substrate appearing in dark contrast at the bottom. EDS-spectra were taken at the indicated points in Figure 1a. The spectrum shown in Figure 1b can be considered as representative for the tribofilm. Besides iron and oxygen, peaks of the elements Cu, Sn, Ba, Si and S are revealed. Since the latter elements were transferred from the pad to the disc, they provide evidence of the pad composition. It is very likely that the pad formulation contained Cu, $BaSO_4$, SnS and or SnS_2. Thus, the EDS-results show that the solid lubricant, tin sulfide in this case, is incorporated in the tribofilm. Graphite-like carbon was also observed, although unfortunately not by STEM-EDS but by HR-TEM [76] or RS [74]. The high Cu signal is partly due to the usage of a copper grid for fixing the TEM lamella. Only the spectrum at point 004 (not shown here) is different compared to the others in the range 002–007. It reveals mainly Zr and O indicating a somewhat larger ZrO_2 particle, in accordance with the findings reported in [76].

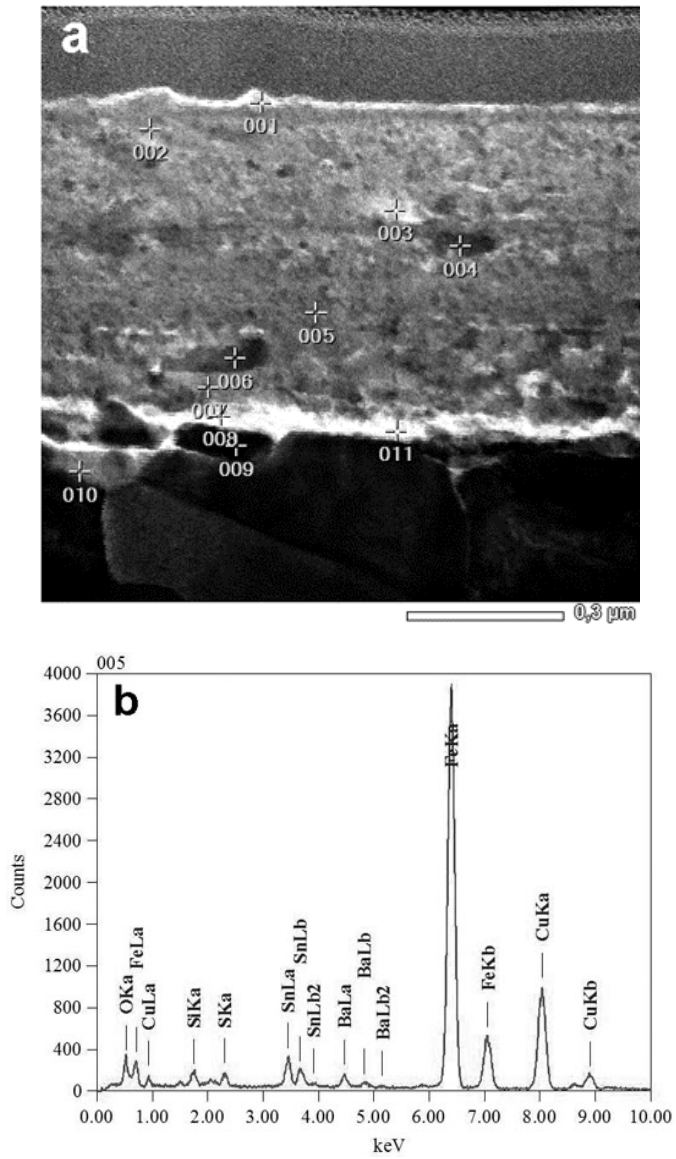

Figure 1. (**a**) Cross-sectional TEM micrograph of a tribofilm at a brake disc surface formed during dynamometer testing against a commercial pad; (**b**) Typical STEM-EDS spectrum taken within the tribofilm at point 005 (without signals from the substrate).

Finally, the following conclusions can be drawn. A fully processed third body formed during multiple braking events and trapped somehow at the interface between pad and disc consists of the following features: Nanocrystalline Fe_3O_4 as the major constituent, nanoparticles of graphite and other soft ingredients distributed homogeneously in the nc-magnetite and eventually submicron-sized abrasives like ZrO_2 or Al_2O_3, also embedded in the magnetite-based matrix. A generalized description of the third body structure would be: A certain amount of soft nanoinclusions (d < 10 nm) and some bigger hard inclusions (50–100 nm) are homogeneously distributed in an agglomerate of brittle oxide nanoparticles. The terms soft and hard indicate whether the corresponding species are softer or harder than the embedding matrix. Copper particles need special consideration. Most investigators observed metallic copper and only rarely copper oxide particles were observed [42,55,59,67,73,76]. In principle, soft metallic particles can adopt the function of solid lubricants like graphite or the metal sulfides. More considerations on copper inclusions in tribofilms are presented in the next section.

4. Modelling of the Sliding Behavior of Tribofilms Formed during Braking

Since usually tribofilms are very thin, showing variation in thickness, incomplete surface coverage, and not well-defined chemical compositions, it is difficult to assess their impact on the frictional performance and sliding behavior. Material modelling can help obtain a better understanding of the impact of film composition and size effects of microstructural features on the sliding behavior. Unfortunately, only very few models are capable of describing processes taking place on the nanometer scale. Whereas Finite Element Modelling (FEM) usually provides only pressure distributions on the macroscopic [82] or, ultimately, on the microscopic scale [83], Molecular Dynamic modelling (MD) is restricted to very limited cases of well-known atomic structures, e.g., rolling of a Ni nanosphere on copper [84]. Other authors applied a Cellular Automata (CA) approach for describing the dynamics of contact patch formation and destruction during automotive braking [85,86]. A Discrete Element Model (DEM), which is well adapted to Godet's concept of the formation, mixing and flow of wear particles was suggested by Fillot *et al.* [87,88]. The most important parameter of this model is adhesion between nanoparticles. Psakhie *et al.* proposed the Movable Cellular Automata (MCA) method which combines concepts of DEM, CA and FEM [89]. The big advantage of this model is that it is not restricted by size, and thus can be adjusted to a large variety of technical as well as geological structures.

Since 2006, the authors have applied the MCA method for simulating the sliding behavior of model-tribofilms similar to the ones observed under real braking conditions. The principles of the approach and a possible combination with FEM modeling were described by Dmitriev *et al.* [90]. The most up to date description of the model, although not its application to friction braking, can be found in [91]. The most important features of the model are shown in Figure 2 and will be explained in the following.

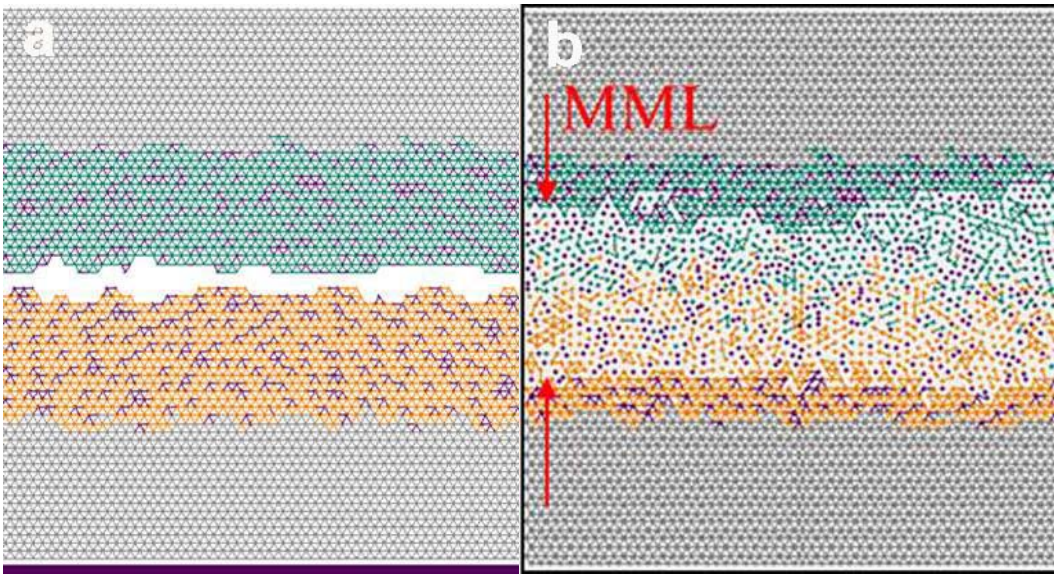

Figure 2. (**a**) Arrangement of linked automata prior to sliding simulation; (**b**) Arrangement of automata after sliding simulation. For further explanations see text. Colors are displayed in the web-version of the article only.

The structure of first bodies and adhering tribofilms is built as two dimensional networks of linked particles, as shown in Figure 2a. Links to neighboring particles are displayed by lines. If we define a particles size of 10 nm, the width of a contact is 0.5 µm and the thickness of the tribofilm (orange or green) is approximately 100 nm. Different materials are depicted by different colors, e.g., grey for the substrates, orange and green for lower and upper tribofilm, respectively, and magenta for soft inclusions in the tribofilms. During sliding simulation, a normal pressure is applied vertically

and a sliding velocity, usually 10 m/s, is applied tangentially. This is done step by step while stresses and strains on each particle are calculated and new positions assigned. Furthermore, the state of linkage is checked by applying a fracture criterion. In the example shown in Figure 2, most of the links between particles were broken within zones at both sides of the interface. The two zones together represent the so-called Mechanically Mixed Layer (MML), because particles from both sides of the interface are mixed within this layer. Furthermore, since the particles within this layer are mostly not linked to their neighbors, they can move almost freely in tangential direction. This is an important feature, because such movement leads to smooth sliding with low friction and velocity accommodation between moving and fixed first bodies. Unlinked particles which are leaving the contact zone at one side are reintroduced on the other side. Thus, periodic boundary conditions are realized.

The main objective of many parameter studies performed during the last 10 years was to find conditions leading to MML-formation at a friction level which is still suitable for brake application.

Table 4 shows the progress made during previous systematic MCA-studies.

5. Discussion

The advantage of modelling is that the impact of structural as well as external parameters can be studied systematically. The disadvantage is that the complexity of structures is limited and mechanisms taking place at different length scales have to be treated separately. Here, only nanoscopic sliding mechanisms were considered. This is justified if sliding occurs within an approximately 100 nm thick surface film which is continuously screening the first bodies. Since wear cannot be neglected, it is necessary to assume that a dynamic equilibrium between film destruction and restitution is taking place. Conditions leading to MML-formation during modelling indicate that a steady state has been reached under which, at least for some time, sliding is determined by particle flow without further destruction of the tribofilm. During a period of particle flow, the COF-fluctuations between time steps are reduced considerably, although the mean COF is not changed. The situation is different for structures which do not show MML-formation. In that case, the tribofilm will be destroyed and removed completely during a sliding simulation within a modelling interval of typically 0.5 μs (2,000,000 time steps). This corresponds to higher wear rates and COF-instabilities not only between the time steps of modelling, but also during practically relevant time intervals of a tribological test procedure.

According to the modelling results shown in Table 4, neither pure metal-on-metal nor oxide-on-oxide contact situations provide MML-formation and corresponding smooth sliding. Only if the oxide is mixed with at least 13 vol % graphite sliding becomes smooth and the COF drops to 0.35 at ambient temperature and high normal pressure [92]. Although most systematic studies have been made while assuming graphite as soft ingredient of the tribofilms, graphite must not be considered as the only species producing this effect. It has been shown that soft copper particles behave similar as graphite [73], and even copper clusters with diameters of 50 nm may substitute halve of the graphite and still provide smooth sliding of the corresponding tribofilm [93]. These results imply that any other constituent will produce a similar effect provided it is significantly softer than the magnetite matrix of the tribofilm. Since all of the metal sulfide solid lubricants considered by Melcher *et al.* [26] are softer than the magnetite, they will show similar effects as the graphite during sliding simulations. The modelling results provide an explanation why the mixing of soft pad ingredients with magnetite, the major wear product from the brake disc, results in smooth sliding at a COF of at least 0.35. Furthermore, it was shown that the COF increases by adding approximately 5 vol % of a hard nanoconstituent, e.g., ZrO_2, SiC or Al_2O_3 [94,95], or by a decrease of the applied pressure [91,92]. Thus, smooth sliding within a COF-range of 0.35–0.5 is predicted by the model for tribofilm nanostructures fulfilling the mentioned requirements.

Table 4. MCA modelling results of model structures containing the essential constituents of real tribofilms formed during automotive braking (chronological order).

Reference	Modeled Structures (vol %) M: Magnetite, C: Graphite	Results (beyond Already Known)	Comments
[65] 2007	1. M + 27C/M + 27C 2. steel/steel 3. steel/cast iron 4. M + 13C + 5Al_2O_3/ ...	1. MML formed, COF = 0.3–0.4 2. no MML, COF = 0.8–0.9 3. no MML, crack at graphite lamella 4. MML formed, COF = 0.45–0.5	1., 4.: High COF fluctuations. Modeling parameters not yet optimized.
[91] 2008	M + xC/M + xC, C = 5–27 Pressure variation: 15–53 MPa	C = 5: no MML, unstable sliding, COF = 0.5 C = 27: MML, smooth sliding, COF = 0.3. Decreasing COF with increasing pressure correlated with MML-thickness	COF = $f(p)$ can explain lower COF compared to [65].
[96] 2008	M + 5C/M + 5C M + 27C/M + 27C	Some more graphite distributions tested. Same quantitative results as [91]	No difference of mean COF.
[90] 2008	1. M + 5C-agglomerates/M + 5C-agglomerates 2. M/M 3. Variants of St/St 4. St/pure graphite layer	1. No MML, unstable sliding, COF = 0.4 2. No MML, unstable sliding, COF = 0.4 3. No MML, unstable sliding, COF = 0.5–0.8 4. MML formed, COF = 0.25	*p*-range: 20–230 MPa. Different for 1., 2., 3. And 4.
[97] 2008	M/M at different pressures	COF = 0.6 at 30 MPa drops to COF = 0.4 at 50 MPa, although no MML is formed	Similar result for M + 5C.
[98] 2010	Impact of graphite concentration (0%–30%) and pressure (15–55 MPa)	Data showing pressure dependency of COF for graphite contents: 0%, 5.5%, 13%, 17.5%, 27% in Fe_3O_4-based tribofilms	Visualization of particle velocity vectors.
[73] 2010	1. Nc-copper instead of steel as substrate material. 2. 27C of tribofilms substituted by soft Cu 3. 5.5C of tribofilms substituted by Cu	1. no impact on COF compared to steel substrate. 2. MML formed at 35MPa, COF = 0.4 slightly higher than with graphite (0.3) 3. No MML, unstable sliding, COF = 0.5 like for 5.5C	Prerequisite for similar behavior as graphite: Recrystallized Cu, assumed to form at high T.
[93] 2011	M + 5.5C + 5.5Cu-clusters/M + 5.5C + 5.5Cu-clusters	Similar behavior as M + 11C, *i.e.*, MML formed, Cu-clusters dissolved within MML	Cu-clusters observed in [73].
[94] 2011	1. M + 13C + 5SiC-clusters/ ... 2. M + 13C as agglomerates instead of compact films	1. MML formed, but clusters not dissolved. 2. Similar MML formation as for compact films	Good correlation with experiments.
[99] 2012	M + 13C agglomerates sliding against each other, p = 30 MPa	Similar COF as compact films	[94] confirmed.
[95] 2012	1. M + 13C + 10SiC-clusters/ ... 2. Different hard Substrates: Cast iron, SiC, Al_2O_3 3. M + 5.5C + 7.5Cu-cluster/ ...	1. COF = 0.4. No further increase compared to 5SiC [94] 2. No impact on COF 3. MML formed, smooth sliding, COF = 0.4	Beneficial effect of Cu-clusters predicted.
[76] 2012	1. M/M 2. M + 27C/M + 27C	Visualization of particle movement (velocity vectors) for the two structures.	Review of other structures.
[100] 2013	Pressure dependencies for: 1. M/M 2. M + 5.5C/M + 5.5C 3. C/C	1. no pressure dependency of COF found. 2. transition from 0.6 to 0.4 at 35 MPa 3. 40) gradual decrease from 0.35 to 0.15	1. contra [94] 2. similar as observed for pure M in [94].
[101] 2014	1. C + xSiC/C + xSiC, x = 0–20 ABCDE COF-pressure dependencies in the range 15–35 MPa	Only slight impact of SiC content on COF as function of p (range 0.35–0.2). More pronounced effect on frictional energy.	Hypothetical study, not related to brakes.
[92] 2014	M + 13C/M + 13C Hypothetic considerations how elevated temperatures may affect mechanical properties of constituents and sliding behavior.	If the temperatures are high enough to make the oxide ductile, the model predicts a change of the tribological behavior: Increasing COF-pressure dependency predicted with increasing temperature. COF may drop from 0.35 to 0.2 at p = 40 MPa.	Velocity reduction from 10 to 1 m/s: no difference of final structure and COF.
[78] 2014	Summary of previous findings	The increase of COF during a stop braking event can be explained by linking MCA-results with patch dynamics [85,86,102]	Loose wear particles play an important role.

A further question is whether the effect of solid lubricants on smooth sliding behavior will also work at elevated temperatures. This can be expected as long as the magnetite is still hard and brittle and the oxides formed from the sulfides are still soft compared to the magnetite. The latter can be expected

for Sb_2O_3 and PbO, but it is not so clear for Sb_2O_4, SnO, SnO_2, MoO_3 and Bi_2O_3 [26]. In the latter cases, the hardness of the oxides approaches that of magnetite. Thus, the effect of initiating smooth sliding conditions might get lost. On the other hand, the experience of many pad manufacturers, namely that metal sulfides provide good fade and wear resistance at elevated temperatures (Table 3), suggests that a similar mechanism may operate as at ambient temperature conditions. This implies that at least part of the metal oxides formed from the sulfides is softer than the magnetite in the temperature range usually responsible for fading effects (>400 °C, see references in Table 1). Hot hardness tests of pure magnetite and the relevant oxides formed from the sulfides at elevated temperatures would be necessary to check this hypothesis.

For the magnetite-graphite system, modelling with a wide range of hypothetical high temperature material properties showed that in principal similar mechanisms occur irrespective of temperature, although with slightly changed quantitative data of the pressure dependencies of COF [92]. In the latter case, it was assumed that magnetite softens and undergoes a brittle-ductile transition while the strength of graphite was considered to be nearly independent of temperature.

A completely different explanation of increased fade resistance can be derived hypothetically if we assume that the oxides formed from the sulfides retain their hardness at elevated temperatures whereas the magnetite undergoes a brittle-ductile transition. Then, an inversion of the microstructure may occur with Sn-, Bi- or Mo-oxides forming hard inclusions within the softened magnetite matrix. Such a film would be comparable to the one studied theoretically in [101]. Thus, smooth sliding at a reduced but stable COF-level can be expected. This is the behavior which frequently is observed while performing fading cycles during dynamometer testing of real brake couples. Although the role of soft inclusions in the sliding mechanism of thin nanostructured tribofilms provides a good explanation for many observations even quantitatively, other mechanisms operating at different length scales may play a role as well. Basically, in terms of size there are two types of particles which are present at the sliding interfaces and, thus, will somehow determine the sliding behavior. The first type corresponds to pad ingredients torn out from the composite due to degradation of the phenolic resin binder. They will still have their original size, usually 10–100 µm. If the gap between first bodies is large enough, such particles can flow along the interface until they are trapped in a surface depression or released to the environment. Unfortunately, we have no information about the impact of flowing micro-particles on the sliding behavior. On the other hand, it is not so unlikely to assume that they might behave similarly to the nanocrystalline multi-phase third body. Anyway, a certain fraction of particles is fragmented by multiple collisions and mixed with the nanocrystalline iron oxide formed by tribooxidation of the disc. Only the latter product can form the thin tribofilms which have the ability to screen the first body surfaces. Thus, the modeled contact sites represent only part of the global contact situation. Furthermore, it should be kept in mind that continuous formation, destruction and reformation of films as well as wear particle production, flow and fragmentation leads to permanent changes of local conditions with time. Thus, predictive modelling for the whole brake system as a function of time is not possible. Nevertheless, if tribofilm formation is considered as crucial for good brake performance properties, the modeling results help to understand the reasons and prerequisites for smooth sliding, wear reduction and COF-stabilization in a range which is suitable for brake applications.

6. Conclusions

Although using solid lubricants as additives for friction composites seems to be somehwhat conflicting, it is common practice. The objective of this review article was to find out why this is so.

A first literature review evaluated experiences of brake pad manufacturers. It turned out that usage of only one solid lubricant additive usually did not yield satisfactory results. In fact, it was necessary to find the right balance between two or more species during an optimization process.

A second review considered results of tribofilm characterization. The films were mostly formed during dynamometer testing simulating real braking conditions. Commercial brake pads were applied against cast iron discs. Thus, a broad variety of different pad formulations were taken into account. Striking similarities between the different systems were revealed. The films consisted mainly of

iron oxide Fe_3O_4, but most of the pad ingredients could be identified as well, although usually only with minor amounts. Besides the magnetite-based films with nanocrystalline structure, micron- or submicron-sized particles of different pad constituents were frequently observed as well, especially in the form of dust particles.

A third review compiled modeling results related to sliding simulations of nanostructures resembling the ones observed for real tribofilms. Although only partial simple systems could be realized, the behavior of more complex systems could be assessed by stitching the results together. After generalization, the following conclusions were drawn: For providing smooth sliding in a COF range of 0.35–0.5, a volume fraction of at least 13% of soft nanoparticles should be embedded in the nanocrystalline magnetite film. If half of the particles are incorporated as clusters, the same effect is observed as for homogeneously embedded particles. Additional hard particle clusters do not disturb the smooth sliding behavior provided that they are completely embedded in the magnetite matrix. As long as solid lubricant additions are softer than the magnetite matrix, they will foster smooth sliding behavior. According to this model, the oxides formed from metal sulfides should be softer than the magnetite even at elevated temperatures, under conditions when the additives prevent fading (undesired COF-decrease) and excessive wear. Unfortunately, hot hardness data of the relevant oxides are not yet available in order to prove this hypothesis.

Acknowledgments: This work was funded by the German Research Foundation (DFG) contract No. OS77/19-1, and partly supported by the RFBR No. 14-08-91330 and the TSU Academic D.I. Mendeleev Fund Program No. 8.1.18.2015. The authors would also like to thank C. Prietzel (formerly BAM, now Institute for Colloidal Chemistry, University Potsdam) for providing not yet published TEM-results.

Author Contributions: Werner Österle surveyed the literature and prepared the manuscript, Andrey I. Dmitriev provided modeling results.

Conflicts of Interest: The authors declare no conflict of interest.

References

1. Zhmud, B.; Pasalskiy, B. Nanomaterials in Lubricants: An industrial perspective on current research. *Lubricants* **2013**, *1*, 95–101. [CrossRef]
2. Zhang, Z.J.; Simionesie, D.; Schaske, C. Graphite and hybrid nanomaterials as lubricant additives. *Lubricants* **2014**, *2*, 44–65. [CrossRef]
3. Yazawa, S.; Minami, I.; Prakash, B. Reducing friction and wear of tribological systems through hybrid tribofilm consisting of coating and lubricants. *Lubricants* **2014**, *2*, 90–112. [CrossRef]
4. Braun, D.; Greiner, C.; Schneider, J.; Gumbsch, P. Efficiency of laser surface texturing in the reduction of friction under mixed lubrication. *Tribol. Int.* **2014**, *77*, 142–147. [CrossRef]
5. Alberdi, A.; Hatto, P.; Diaz, B.; Csillag, S. Tribological behavior of nanocomposite coatings based on fullerene-like structures. *Vacuum* **2011**, *85*, 1087–1092. [CrossRef]
6. Thomas, P.; Mansot, J.L.; Molza, A.; Begarin, F.; Dubois, M.; Guerin, K. Friction properties of fluorinated graphitized carbon blacks. *Tribol. Lett.* **2014**, *56*, 259–271. [CrossRef]
7. Steiner, L.; Bouvier, V.; May, U.; Hegadekatte, V.; Huber, N. Modeling of unlubricated oscillating sliding wear of DLC-coatings considereding surface topography, oxidation and graphitization. *Wear* **2010**, *268*, 1184–1194. [CrossRef]
8. Martin, J.M.; Pascal, H.; Donnet, C.; Le Mogne, T.; Loubet, J.L.; Epicier, T. Superlubricity of MoS_2: Crystal orientation mechanisms. *Surf. Coat. Technol.* **1994**, *68*, 427–432. [CrossRef]
9. Morita, Y.; Onodera, T.; Suzuki, A.; Sahnoun, R.; Koyama, M.; Tsuboi, H.; Hatakeyama, N.; Endou, A.; Takaba, H.; Kubo, M.; *et al*. Development of a new molecular dynamics method for tribochemical reaction and its application to formation dynamics of MoS_2 tribofilm. *Appl. Surf. Sci.* **2008**, *254*, 7618–7621. [CrossRef]
10. Colas, G.; Saulot, A.; Godeau, C.; Michel, Y.; Berthier, Y. Decrypting third body flows to solve dry lubrication issue-MoS_2 case study under ultrahigh vacuum. *Wear* **2013**, *305*, 192–204. [CrossRef]
11. An, V.; Irtegov, Y.; de Izarra, C. Study of tribological properties of nanolamellar WS2 and MoS_2 as additives to lubricants. *J. Nanomater.* **2014**. Available online: http://dx.doi.org/10.1155/2014/865839 (accessed on 25 February 2016).

12. Rapoport, L.; Leshchinsky, V.; Lvovsky, M.; Lapsker, I.; Volovik, Y.; Feldman, Y.; Popovitz-Biro, R.; Tenne, R. Superior tribological properties of powder materials with solid lubricant nanoparticles. *Wear* **2003**, *255*, 794–800. [CrossRef]
13. Martin, J.M.; Onodera, T.; Minfray, C.; Dassenoy, F.; Miyamoto, A. The origin of anti-wear chemistry of ZDDP. *Faraday Discuss.* **2012**, *156*, 311–323. [CrossRef] [PubMed]
14. Kunze, T.; Posselt, M.; Gemming, S.; Seifert, G.; Konicek, R.; Carpick, R.W.; Pastewka, L.; Moseler, M. Wear, plasticity, and rehybridization in tetrahedral amorphous carbon. *Tribol. Lett.* **2014**, *53*, 119–126. [CrossRef]
15. Godet, M. The third body approach: A mechanical view of wear. *Wear* **1984**, *100*, 437–452. [CrossRef]
16. Blau, P.J. *Compositions Functions and Testing of Friction Brake Materials and Their Additives*; Technical Report 64; Oak Ridge National Laboratory: Oak Ridge, TN, USA, 2001.
17. Goudier, M.; Berthier, Y.; Jacquemard, P.; Rousseau, B.; Bonnamy, S.; Estrade-Szwarckopf, H. Mass spectrometry during C/C composite friction: Carbon oxidation associated with high friction coefficient and high wear rate. *Wear* **2004**, *256*, 1082–1087. [CrossRef]
18. Kasem, H.; Bonnamy, S.; Berthier, Y.; Dufrenoy, P.; Jacquemard, P. Tribological, physicochemical and thermal study of the abrupt friction transition during C/C composite friction. *Wear* **2009**, *267*, 846–852. [CrossRef]
19. Stadler, Z.; Krnel, K.; Kosmac, T. Friction and wear of sintered metallic brake linings on a C/C-SiC composite brake disc. *Wear* **2008**, *265*, 278–285. [CrossRef]
20. Cho, M.H.; Ju, J.; Kim, J.; Jang, H. Tribological properties of solid lubricants (graphite, Sb_2S_3, MoS_2) for automotive brake friction materials. *Wear* **2006**, *260*, 855–860. [CrossRef]
21. Ram-Prabhu, T. Effects of solid lubricants, load, and sliding speed on the tribological behavior of silica reinforced composites using design of experiments. *Mater. Des.* **2015**, *77*, 149–160. [CrossRef]
22. Chen, B.; Bi, Q.; Yang, J.; Xia, Y.; Hao, J. Tribological properties of solid lubricants (graphite, h-BN) for Cu-based P/M friction composites. *Tribol. Int.* **2008**, *41*, 1145–1152. [CrossRef]
23. Su, L.; Gao, F.; Han, X.; Fu, R.; Zhang, E. Tribological behavior of copper-graphite powder third body on copper-based friction materials. *Tribol. Lett.* **2015**, *60*, 30. [CrossRef]
24. Li, X.; Gao, Y.; Xing, J.; Wang, Y.; Fang, L. Wear reduction mechanism of graphite and MoS_2 in epoxy composites. *Wear* **2004**, *257*, 279–283. [CrossRef]
25. Pan, G.; Guo, Q.; Ding, J.; Zhang, W.; Wang, X. Tribological behaviors of graphite/epoxy two phase composite coatings. *Tribol. Int.* **2010**, *43*, 1318–1325. [CrossRef]
26. Melcher, B.; Faullant, P. *A Comprehensive Study of Chemical and Physical Properties of Metal Sulfides*; SAE Technical Paper 2000-01-2757; SAE: Warrendale, PA, USA, 2000; pp. 39–49.
27. Gudmand-Hoyer, L.; Bach, A.; Nielsen, G.T.; Morgen, P. Tribological properties of automotive disc brakes with solid lubricants. *Wear* **1999**, *232*, 168–175. [CrossRef]
28. Matejka, V.; Lu, Y.; Matekova, P.; Smetana, B.; Kukutschova, J.; Vaculik, M.; Tomasek, V.; Zla, S.; Fan, Y. Possible stibnite transformation at the friction surface of the semi-metallic friction composites designed for car brake linings. *Appl. Surf. Sci.* **2011**, *258*, 1862–1868. [CrossRef]
29. Kim, S.J.; Cho, M.H.; Cho, K.H.; Jang, H. Complementary effects of solid lubricants in the automotive brake lining. *Tribol. Int.* **2007**, *40*, 15–20. [CrossRef]
30. Jang, H.; Kim, S.J. The effects of antimony trisulfide and zirconium silicate in the automotive brake friction material on friction characteristics. *Wear* **2000**, *239*, 229–236. [CrossRef]
31. Holinski, R. Improvement of comfort of friction brakes. In Proceedings of the World Tribology Congress, Vienna, Austria, 3–7 September 2001; Franek, F., Bartz, W.J., Pauschitz, A., Eds.; The Austrian Tribological Society: Vienna, Austria, 2001.
32. Jang, H.; Lee, J.S.; Fash, J.W. Compositional effects of the brake friction material on creep groan phenomena. *Wear* **2001**, *251*, 1477–1483. [CrossRef]
33. Mutlu, I.; Eldogan, O.; Findik, F. Tribological properties of some phenolic composites suggested for automotive brakes. *Tribol. Int.* **2006**, *39*, 317–325. [CrossRef]
34. Yi, G.; Yan, F. Mechanical and tribological properties of phenolic resin-based friction composites filled with several inorganic fillers. *Wear* **2007**, *262*, 121–129. [CrossRef]
35. Abdel-Rahim, Y.M.; Darwish, S.M. Generalized braking charakteristics of friction pad synthetic graphite composites. *Tribol. Int.* **2010**, *43*, 838–843. [CrossRef]

36. Kolluri, D.K.; Boidin, X.; Desplanques, Y.; Degallaix, G.; Ghosh, A.K.; Kumar, M.; Bijwe, J. Effect of natural graphite particle size in friction materials on thermal localization phenomenon during stop-braking. *Wear* **2010**, *268*, 1472–1482. [CrossRef]
37. Yun, R.; Filip, P.; Lu, Y. Performance and evaluation of eco-friendly brake friction materials. *Tribol. Int.* **2010**, *43*, 2010–2019. [CrossRef]
38. Uexküll, O.; Skerfving, S.; Doyle, R.; Braungart, M. Antimony in brake pads—A carcinogenic component? *J. Clean. Prod.* **2005**, *13*, 19–31. [CrossRef]
39. Morbach, M.; Paul, H.G.; Severit, P. Systematic approach for structured product development of copper free friction materials. In Proceedings of the EuroBrake 2012, Dresden, Germany, 16–18 April 2012.
40. Martinez, A.M.; Echeberria, J.; Di Loreto, A.; Zanon, M.; Rampin, I. Joint development of copper-free fow steel brake pads for light vehicles. In Proceedings of the EuroBrake 2014, Lille, France, 16–18 May 2014.
41. Martinez, A.M.; Echeberria, J.; Zanon, M.; Di Loreto, A. Characterization of the chemical reactions between solid lubricants and metal powders in low metallic brake pads during braking. In Proceedings of the EuroBrake 2015, Dresden, Germany, 4–6 May 2015.
42. Verma, P.C.; Menapace, L.; Bonfanti, A.; Ciudin, R.; Gialanella, S.; Straffelini, G. Braking pad-disc system: Wear mechanisms and formation of wear fragments. *Wear* **2015**, *322–323*, 251–258. [CrossRef]
43. Jacko, M.G.; DuCharme, R.T.; Somers, J.H. Brake and clutch emissions generated during vehicle operation. In Proceedings of the SAE Automobile Engineering Meeting, Detroit, MI, USA, 14–18 May 1973; Society of Automotive Engineers INC: New York, NY, USA, 1973.
44. Bark, L.S.; Moran, D.; Percival, S.J. Polymer changes during friction material performance. *Wear* **1977**, *41*, 309–314. [CrossRef]
45. Libsch, T.A.; Rhee, S.K. Microstructural changes in semimetallic disc brake pads created by low temperature dynamometer testing. *Wear* **1978**, *46*, 203–212. [CrossRef]
46. Jacko, M.G. Physical and chemical changes of organic disc pads in service. *Wear* **1978**, *46*, 163–175. [CrossRef]
47. Scieszka, S.F. Tribological phenomena in steel-composite brake material friction pairs. *Wear* **1980**, *64*, 367–378. [CrossRef]
48. Jacko, M.G.; Tsang, P.H.S.; Rhee, S.K. Wear debris compaction and friction film formation of polymer composites. *Wear* **1989**, *133*, 23–38. [CrossRef]
49. Wirth, A.; Eggleston, D.; Whitaker, R. A fundamental tribochemical study of the third body layer formed during automotive friction braking. *Wear* **1994**, *179*, 75–81. [CrossRef]
50. Singer, I. Mechanics and chemistry of solids in sliding contact. *Langmuir* **1996**, *12*, 4486–4491. [CrossRef]
51. Filip, P.; Wright, M.A. Characterization of composite materials for automotive braking industry. *Prakt. Met. Sonderband* **1999**, *30*, 449–456.
52. Eriksson, M.; Jacobson, S. Tribological surfaces of organic brake pads. *Tribol. Int.* **2000**, *33*, 817–827. [CrossRef]
53. Garg, B.D.; Cadle, S.H.; Mulawa, P.A.; Groblicki, P.J. Brake wear particulate matter emissions. *Environ. Sci. Technol.* **2000**, *34*, 4463–4469. [CrossRef]
54. Eriksson, M.; Lord, J.; Jacobson, S. Wear and contact conditions of brake pads: Dynamical *in situ* studies of pad on glass. *Wear* **2001**, *249*, 272–278. [CrossRef]
55. Filip, P.; Weiss, Z.; Rafaja, D. On friction layer formation in polymer matrix composite materials for brake applications. *Wear* **2002**, *252*, 189–198. [CrossRef]
56. Kharrazi, Y.H.K.; Österle, W. The microstructure of brake lining materials containing asbestos and possible asbestos substitudes. *Prakt. Metallogr.* **2002**, *39*, 542–556.
57. Ingo, G.M.; Uffizi, M.D.; Falso, G.; Bultrini, G.; Padeletti, G. Thermal and microchemical investigation of automotive brake pad wear residues. *Thermochim. Acta* **2004**, *418*, 61–68. [CrossRef]
58. Mosleh, M.; Blau, P.J.; Dumitrescu, D. Characterisation and morphology of wear particles from laboratory testing of disk brake materials. *Wear* **2004**, *256*, 1128–1134. [CrossRef]
59. Österle, W.; Urban, I. Friction layers and friction films on PMC brake pads. *Wear* **2004**, *257*, 215–226. [CrossRef]
60. Österle, W.; Bettge, D. A comparison of methods for characterizing brake lining surfaces. *Prakt. Metallogr.* **2004**, *41*, 494–504.
61. Cho, M.H.; Cho, K.H.; Kim, S.J.; Kim, D.H.; Jang, H. The role of transfer layers on friction characteristics in the sliding interface between friction materials against gray iron brake disks. *Tribol. Lett.* **2005**, *20*, 101–108. [CrossRef]

62. Österle, W.; Dmitriev, A.I.; Urban, I. Characterization of up to date brake friction materials. In Proceedings of the International Workshop on Advances in Asbestos-Free Friction Compositers—I (IWAAFC-1), New Dehli, India, 5–6 January 2006; Bijwe, J., Ed.; ITMMEC, Indian Institute of Technology: Dehli, India, 2006; pp. 21–35.
63. Österle, W.; Urban, I. Third body formation on brake pads and rotors. *Tribol. Int.* **2006**, *39*, 401–408. [CrossRef]
64. Cristol-Bulthe, A.L.; Desplanques, Y.; Degallaix, G.; Berthier, Y. Mechanical and chemical investigation of the temperature influence on the tribological mechanisms occurring in OMC/cast iron friction contact. *Wear* **2008**, *264*, 815–825. [CrossRef]
65. Österle, W.; Kloß, H.; Urban, I.; Dmitriev, A.I. Towards a better understanding of brake friction materials. *Wear* **2007**, *263*, 1189–1201. [CrossRef]
66. Roubicek, V.; Raclavska, H.; Juchelkova, D.; Filip, P. Wear and environmental aspects of composite materials for automotive braking industry. *Wear* **2008**, *265*, 167–175. [CrossRef]
67. Österle, W.; Dörfel, I.; Prietzel, C.; Rooch, H.; Cristol-Bulte, A.L.; Degallaix, G.; Desplanques, Y. A comprehensive study of third body formation at the interface between a brake pad and brake disc during the final stage of a pin-on-disc test. *Wear* **2009**, *267*, 781–788. [CrossRef]
68. Österle, W.; Bresch, H.; Dörfel, I.; Prietzel, C.; Seeger, S.; Fink, C.; Giese, A.; Walter, J. Surface film formation and dust generation during brake performance tests. In Proceedings of the Conference on Braking 2009, York, UK, 9–10 June 2009; Institution of Mechanical Engineers, Chandos Publishing: Oxford, UK, 2009; pp. 29–38.
69. EL-Tayeb, N.S.M.; Liew, K.W. On dry and wet sliding performance of potentially new frictional brake pad materials for automotive industry. *Wear* **2009**, *266*, 275–287. [CrossRef]
70. Kukutschova, J.; Roubicek, V.; Maslan, M.; Jancik, D.; Slovak, V.; Malachova, K.; Pavlickova, Z.; Filip, P. Wear performance and wear debris of semimetallic automotive brake materials. *Wear* **2010**, *268*, 86–93. [CrossRef]
71. Österle, W.; Prietzel, C.; Dmitriev, A.I. Investigation of surface film nanostructure and assessment of its impact on friction force stabilization during automotive braking. *Int. J. Mater. Res.* **2010**, *101*, 669–675. [CrossRef]
72. Österle, W.; Bresch, H.; Dörfel, I.; Fink, C.; Giese, A.; Prietzel, C.; Seeger, S.; Walter, J. Examination of airborne brake dust. In Proceedings of the 6th European Conference on Braking JEF 2010, Lille, France, 24–25 November 2010; pp. 55–60.
73. Österle, W.; Prietzel, C.; Kloß, H.; Dmitriev, A.I. On the role of copper in brake friction materials. *Tribol. Int.* **2010**, *43*, 2317–2326. [CrossRef]
74. Hinrichs, R.; Vasconcellos, M.A.Z.; Österle, W.; Prietzel, C. A TEM snapshot of magnetite formation in brakes: The role of the disc's cast iron graphite lamellae in third body formation. *Wear* **2011**, *270*, 365–370. [CrossRef]
75. Österle, W.; Dmitriev, A.I. Functionality of conventional brake friction materials—Preceptions from findings observed at different length scales. *Wear* **2011**, *271*, 2198–2207. [CrossRef]
76. Österle, W.; Dmitriev, A.I.; Kloß, H. Does ultra-mild wear play any role for dry friction applications, such as automotive braking? *Faraday Discuss.* **2012**, *156*, 159–171. [CrossRef] [PubMed]
77. Fernandes, G.P.; Haertel, W.; Zanotto, P.S.; Sinatora, A. Inluence of mild and severe wear condition in the formation and stability of friction film in clutch system. *Wear* **2013**, *302*, 1384–1391. [CrossRef]
78. Österle, W.; Dmitriev, A.I. Some considerations on the role of third bodies during automotive braking. *SAE Int. J. Passeng. Cars Mech. Syst.* **2014**, *7*, 1287–1294. [CrossRef]
79. Österle, W.; Orts-Gil, G.; Gross, T.; Deutsch, C.; Hinrichs, R.; Vasconcellos, M.A.Z.; Zoz, H.; Yigit, D.; Sun, X. Impact of high energy ball milling on the nanostructure of magnetite-graphite and magnetite-graphite-molybdenum disulphide blends. *Mater. Charact.* **2013**, *86*, 28–38. [CrossRef]
80. Österle, W.; Deutsch, C.; Gradt, T.; Orts-Gil, G.; Schneider, T.; Dmitriev, A.I. Tribological screening tests for the selection of raw materials for automotive brake pad formulations. *Tribol. Int.* **2014**, *73*, 148–155. [CrossRef]
81. Häusler, I.; Dörfel, I.; Peplinski, B.; Dietrich, P.M.; Unger, W.E.S.; Österle, W. Comprehensive characterization of a tribofilm produced by ball milling of a model tribo system. *Mater. Charact.* **2016**, *111*, 183–192. [CrossRef]
82. Söderberg, A.; Andersson, S. Simulation of wear and contact pressure distribution at the pad-to-rotor interface in a disc brake using general purpose finite element analysis software. *Wear* **2009**, *267*, 2243–2251. [CrossRef]
83. Dick, T.; Cailletaud, G. Analytic and FE based estimations pf the coefficient of friction of composite surfaces. *Wear* **2006**, *260*, 1305–1316. [CrossRef]

84. Lee, W.G.; Cho, K.H.; Jang, H. Molecular dynamics simulation of rolling friction using nanosize spheres. *Tribol. Lett.* **2009**, *33*, 37–43. [CrossRef]
85. Ostermeyer, G.P.; Müller, M. New insights into the tribology of brake systems. *Automob. Eng.* **2008**, *222*, 1167–1200. [CrossRef]
86. Wahlström, J. A Study of Airborne Wear Particles from Automotive Disc Brakes. Ph.D. Thesis, Royal Institute of Technology, Stockholm, Sweden, 2011.
87. Fillot, N.; Iordanoff, I.; Berthier, Y. Wear modelling and the third body concept. *Wear* **2007**, *262*, 949–957. [CrossRef]
88. Fillot, N.; Iordanoff, I.; Berthier, Y. Modelling third body flows with a discrete element method—A tool for understanding wear with adhesive particles. *Tribol. Int.* **2007**, *40*, 973–981. [CrossRef]
89. Psakhie, S.G.; Horie, Y.; Ostermeyer, G.P.; Korostelev, S.Y.; Smolin, A.Y.; Shilko, E.V.; Dmitriev, A.I.; Blatnik, S.; Špegel, M.; Zavšek, S. Movable cellular automata method for simulating materials with mesostructured. *Theor. Appl. Fract. Mech.* **2001**, *37*, 311–334. [CrossRef]
90. Dmitriev, A.I.; Smolin, A.Y.; Psakhie, S.G.; Österle, W.; Kloss, H.; Popov, V.L. Computer modeling of local tribological contacts by the example of the automotive brake friction pair. *Phys. Mesomech.* **2008**, *11*, 73–84. [CrossRef]
91. Dmitriev, A.I.; Österle, W.; Wetzel, B.; Zhang, G. Mesoscale modeling of the mechanical and tribological behavior of a polymer matrix composite based on epoxy and 6 vol % silica nanoparticles. *Comput. Mater. Sci.* **2015**, *110*, 204–214. [CrossRef]
92. Dmitriev, A.I.; Österle, W. Modelling the sliding behaviour of tribofilms forming during automotive braking: Impact of loading parameters and property range of constituents. *Tribol. Lett.* **2014**, *53*, 337–351. [CrossRef]
93. Österle, W.; Dmitriev, A.I.; Kloß, H. Prerequisites for smooth sliding behaviour derived by modelling on the nanometre scale. In Proceedings of the 3rd European Conference on Tribology, Vienna, Austria, 7–9 June 2011; pp. 869–870.
94. Dmitriev, A.I.; Oesterle, W.; Kloss, H. Nano-scale modelling of automotive pad-disc interface. The influence of structure & composition. In Proceedings of the International Conference on BALTRIB 2011, Kaunas, Lithuania, 17–19 November 2011; pp. 236–242.
95. Österle, W.; Dmitriev, A.I.; Kloß, H. Possible impacts of third body nanostructure on friction performance during dry sliding determined by computer simulation based on the method of movable cellular automata. *Tribol. Int.* **2012**, *48*, 128–136. [CrossRef]
96. Österle, W.; Kloß, H.; Dmitriev, A.I. Modeling of friction evolution and assessment of impacts on vibration excitation at the pad-disc interface. In Proceedings of the 26th Annual Brake Colloquium, San Antonio, TX, USA, 12–15 October 2008; pp. 303–311.
97. Dmitriev, A.I.; Österle, W.; Kloß, H. Numerical simulation of mechanically mixed layer formation at local contacts of an automotive brake system. *Trib. Trans.* **2008**, *51*, 810–816. [CrossRef]
98. Dmitriev, A.I.; Österle, W. Modeling of brake pad-disc interface with emphasis to dynamics and deformation of structures. *Tribol. Int.* **2010**, *43*, 719–727. [CrossRef]
99. Dmitriev, A.I.; Österle, W.; Kloß, H.; Orts-Gil, G. A study of third body behaviour under dry sliding conditions. Comparison of nanoscale modelling with experiment. *Estonian J. Eng.* **2012**, *18*, 270–278.
100. Österle, W.; Dmitriev, A.I.; Orts-Gil, G.; Schneider, T.; Ren, H.; Sun, X. Verification of nanometre-scale modelling of tribofilm sliding behaviour. *Tribol. Int.* **2013**, *62*, 155–162. [CrossRef]
101. Österle, W.; Dmitriev, A.I.; Kloß, H. Assessment of sliding friction of a nanostructured solid lubricant film by numerical simulation with the method of movable cellular automata (MCA). *Tribol. Lett.* **2014**, *54*, 257–262.
102. Wahlström, J. A comparison of measured and simulated friction, wear and particle emission of disc brakes. *Tribol. Int.* **2015**, *92*, 503–511.